Chapter 5

Beamformer Based on Quaternion Processes

Jian-wu Tao and Wen-xiu Chang

Additional information is available at the end of the chapter

http://dx.doi.org/10.5772/67859

Abstract

In this chapter, the problem of quaternion beamformer based on linear and widely linear hypercomplex processing is investigated in scenarios, where there exist one signal and one interference that are uncorrelated. First, we introduce brief information about the quaternion algebra and a quaternion model of linear symmetric array with two-component electromagnetic (EM) vector-sensors is presented. Based on array's quaternion model, a quaternion MVDR (QMVDR) beamformer is derived and its performance is analysed. Second, we propose the general expression of a quaternion *semi-widely* linear (QSWL) beamformer and derive its useful implementation and the array's gain expression. Finally, we give the main results of Monte Carlo simulation.

Keywords: quaternion beamforming, hypercomplex processes, widely linear hypercomplex processes, polarization signal processes, EM vector-sensor array

1. Introduction

As an important tool of multidimensional signal processing, the quaternion algebra has been applied to spatio-temporal-polarization beamformer based on an electromagnetic (EM) vector-sensor array [1–5]. The potential advantages of multidimensional signal processing are: (1) the correlation and coupling between each dimension are naturally considered, leading to improved accuracies of signal processing; (2) signals of different geometric nature in different dimensions are being represented as a single signal, leading to reduced complexity of processing approaches. For example, we consider an array consisting of M two-component vector-sensors (If an EM vector-sensor consists of only two components, such as two magnetic loops [6], one electric dipole plus one magnetic loop [7] and two electric dipoles [3], it is referred to a two-component vector-sensor in this chapter.), the output of complex 'long vector' beamformer [8, 9] is $y_c = \mathbf{w}_c^H \boldsymbol{x}_c$ where $\boldsymbol{x}_c = [x_{11}, x_{12}, \ldots x_{M1}, x_{M2}]^T$ is the observed vector of array; $\mathbf{w}_c = [w_{11}, w_{12}, \ldots w_{M1}, w_{M2}]^T$ is a complex weighted vector; the symbol $(.)^H$ denotes the complex conjugation transposition operator. Whereas the output of quaternion-based beamformer [3–5] is $y_h = \mathbf{w}_h^{\Delta} \boldsymbol{x}_h = y_c + j\, y_e$ where

$\boldsymbol{x}_h = [x_{h1}, x_{h2}, \ldots x_{hM}]^T$ is the quaternion-valued, observed vector of array and $x_{hm} = x_{m1} + jx_{m2}$ $(m = 1, \ldots, M)$. $\mathbf{w}_h = [w_{h1}, w_{h2}, \ldots w_{hM}]^T$ is a quaternion-valued, weighted vector and $w_{hm} = w_{m1} + jw_{m2}$ $(m = 1, \ldots, M)$. The symbol $(.)^{\Delta}$ denotes the quaternion conjugation transposition operator and j denotes an imaginary unit of quaternions. Comparing y_h with y_c, we can see that the output of quaternion-based beamformer has one more extra information y_e than the output of complex 'long vector' beamformer. By employing this extra information y_e, we can further improve the performance of beamformer.

In this chapter, our aim is to investigate the beamformer of EM vector-sensor array, based on quaternion processes. First, a QMVDR beamformer and its interference and noise canceller (INC) algorithm are proposed. The output signal to interference-plus-noise ratio (*SINR*) expression of INC algorithm is derived in a scenario where there exist one signal and one interference that are uncorrelated. By analysing the effect of sources parameters on the output *SINR*, the fact is explicitly revealed that even though no separation between the DOA's of the desired signal and interference, the maximum value of output *SINR* can be obtained using the orthogonality between the polarizations of the desired signal and interference. Second, we propose a quaternion *semi-widely* linear beamformer and its useful implementation, i.e., quaternion *semi-widely* linear (QSWL) Generalized sidelobe canceller (GSC). Since the QSWL GSC consists of two-stage beamformers, it has more information than the complex 'long vector' beamformer. The increase in information results in the improvement of the beamformer's performance. By designing the weight vectors of two-stage beamformers, the interference is completely cancelled in the output of QSWL GSC and the desired signal is not distorted.

2. Quaternion algebra and vector-sensor array model

2.1. Quaternion algebra

Quaternion came up in the investigations of constructing multidimensional analogues of the field of complex numbers **C**. The field of quaternion numbers **Q** is also algebra over the field of real numbers **R**. The dimension of this algebra is four, and four basis elements are 1, *i, j* and *k*. In field of quaternion numbers **Q**, following multiplication is satisfied

$$i^2 = j^2 = k^2 = -1;\ ij = k = -ji; jk = i = -kj; ki = j = -ik \tag{1}$$

A quaternion variable $x \in \mathrm{Q}$ has two forms of representation. One form is $x = x_1 + ix_2 + jx_3 + kx_4$, where x_1, x_2, x_3 and x_4 are real coefficients. It is referred to as the **R**-expansion of quaternions. We call x_1 the real/scalar part of x, and it is denoted by $\Re(x)$. $ix_2 + jx_3 + kx_4$ is called the imaginary/vector part of x, and it is denoted by $\Im(x)$. We refer to $x^* = x_1 - ix_2 - jx_3 - kx_4$ as the conjugate of x and $|x| = (x_1^2 + x_2^2 + x_3^2 + x_4^2)^{1/2}$ as the modulus of x. The other form is $x = z_1 + jz_2$, where z_1 and z_2 are complex coefficients. It is called the **C**-expansion of quaternions or *Cayley-Dickson*. $x^* = z_1^* - jz_2$ is the conjugate of x and $|\mathrm{x}| = (|z_1|^2 + |z_2|^2)^{1/2}$ is the modulus of x. Several properties of quaternions are discussed in **Table 1** [10–12].

http://dx.doi.org/10.5772/67859

x and y denotes two quaternions				
Conjugation	**Norm, noted** $\|.\|$	**Inverse, noted** x^{-1}	**Multiplication**	
$xx^*=x^*x=\|x\|^2$	$\|x\| = 0$ if and only if x=0	If $x \neq 0$, $x^{-1}= x^*/\|x\|^2$	$a: \in \mathbf{R}$	$ax = xa$
$\|x\|=\|x^*\|$	$\|xy\| = \|yx\| = \|x\|\|y\|$		$c \in \mathbf{C}$	$jc = c^*j$, $jcj^*=c^*$
$(xy)^*=y^*x^*$	$\|x+y\| \leq \|x\| + \|y\|$		$q \in \mathbf{Q}$	$xq \neq qx$

Table 1. Several properties of quaternions.

2.2. Vector-sensor array model

Consider a scenario with one narrowband, completely polarized source, which is travelling in an isotropic and homogeneous medium, impinges on a uniform linear symmetric array from direction (θ, φ). This array consists of $2M$ two-component vector-sensors, which is depicted in **Figure 1**, and the spacing between the adjacent two vector-sensors is assumed to be half wavelength. All the vector-sensors are indexed by $-M,\ldots, -1,1,\ldots,M$ from left to right.

Let the array centre be the phase reference point, two highly complex series $x_{\mathrm{m1}}(n)$ and $x_{\mathrm{m2}}(n)$ are recorded on first and second components of the mth two-component vector-sensor, respectively. $x_{\mathrm{m1}}(n)$ and $x_{\mathrm{m2}}(n)$ are given by Ward [10]

$$\begin{bmatrix} x_{\mathrm{m1}}(n) \\ x_{\mathrm{m2}}(n) \end{bmatrix} = \begin{bmatrix} a_1(\theta,\varphi,\gamma,\eta) \\ a_2(\theta,\varphi,\gamma,\eta) \end{bmatrix} q_m(\theta,\varphi)s(n) \tag{2}$$

where $0 \leq \theta \leq \pi$ and $0 \leq \varphi < \pi$ denote the incidence source's elevation angle measured from the positive z-axis and the azimuth angle measured from the positive x-axis, respectively. $0 \leq \gamma < \pi/2$ represents the auxiliary polarization angle, and $-\pi \leq \eta < \pi$ signifies the polarization phase difference. $a_1(\theta,\varphi,\gamma,\eta)$ and $a_2(\theta,\varphi,\gamma,\eta)$ are the responses on first and second components of two-component vector-sensor, respectively. The two-component vector-sensor consists of one electric dipole plus one magnetic loop co-aligned along the x-axis, where $a_1(\theta,\varphi,\gamma,\eta) = e^{i\eta}\cos\varphi\cos\theta\sin\gamma - \sin\varphi\cos\gamma$ and $a_2(\theta,\varphi,\gamma,\eta) = -e^{i\eta}\sin\varphi\sin\gamma - \cos\varphi\cos\theta\cos\gamma$ [7] or two magnetic loops co-aligned along the x-axis, where $a_1(\theta,\varphi,\gamma,\eta) = -e^{i\eta}\sin\varphi\sin\gamma - \cos\varphi\cos\theta\cos\gamma$ and $a_2(\theta,\varphi,\gamma,\eta) = e^{i\eta}\cos\varphi\sin\gamma - \sin\varphi\cos\theta\cos\gamma$ [6]. $q_m(\theta,\varphi)$ is the spatial phase factor describing wave-field propagation along the array, and $q_m(\theta,\varphi) = q^*_{-m}(\theta,\varphi)$ due to the

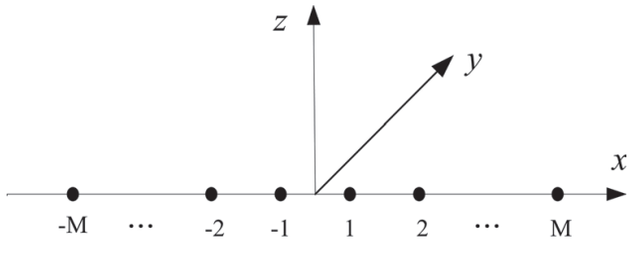

Figure 1. A uniform linear symmetric array.

symmetric structure of array. $s(n)$ is the complex envelope of the waveform, assumed to be a zero-mean, stationary stochastic process.

Using $x_{\mathrm{m1}}(n)$ and $x_{\mathrm{m2}}(n)$ ($m = -M, \ldots, M$), a quaternion-valued series $x_{\mathrm{m}}(n)$ can be constructed in the **C**-expansion of quaternions, as the output of the mth two-component vector-sensor:

$$\begin{aligned} x_m(n) &= x_{m1}(n) + jx_{-m2}(n) = q_m(\theta, \varphi)\Big(a_1(\theta, \varphi, \gamma, \eta) + ja_2(\theta, \varphi, \gamma, \eta)\Big)s(n) \\ &= q_m(\theta, \varphi)P(\theta, \varphi, \gamma, \eta)s(n) \end{aligned} \tag{3}$$

where j denotes an imaginary unit of quaternions. $P(\theta, \varphi, \gamma, \eta)$ is the quaternion-valued response on two-component vector-sensor. This transformation maps the complex series $x_{\mathrm{m1}}(n)$ on scalar and i imaginary fields of a quaternion, and the complex series $x_{\mathrm{m2}}(n)$ is simultaneously mapped to the j and k imaginary fields. When the quaternion-valued additive noise is considered, the quaternion-valued output of the mth two-component vector-sensor is given by

$$x_m(n) = q_m(\theta, \varphi)P(\theta, \varphi, \gamma, \eta)s(n) + n_m(n) \tag{4}$$

where $n_m(n) = n_{m1}(n) + jn_{-m2}(n)$. $n_{m1}(n)$ is the complex-valued additive noises recorded on first component of the mth vector-sensor and $n_{-m2}(n)$ is the complex-valued additive noises recorded on second component of the mth vector-sensor, which are assumed to be zero mean, Gaussian noise with identical covariance σ_n^2. And it is assumed that $n_m(n)$ and $n_n(n)$, where $m \neq n$, are uncorrelated.

3. Quaternion MVDR (QMVDR) beamformer

It is assumed that two uncorrelated, completely polarized plane-waves impinge on an array with $2M$ two-component vector-sensor. One is the desired signal characterized by its arrival angles (θ_s, φ_s) and polarization parameters (γ_s, η_s); the other is the interference characterized by its arrival angles (θ_i, φ_i) and polarization parameters (γ_i, η_i). Assumed interference's DOA and polarization are unknown but signal's DOA and polarization are known or may be priorly estimated from techniques. Thus, the quaternion-valued measurement vector of array can be written as

$$\boldsymbol{x}(n) = [x_{-M}(n), \cdots, x_M(n)]^T = \boldsymbol{v}_s s_s(n) + \boldsymbol{v}_i s_i(n) + \boldsymbol{n}(n) \tag{5}$$

where $\boldsymbol{n}(n) = [n_{-M}(n), \cdots, n_M(n)]^T$ denotes the quaternion-valued additive noise vector. $\boldsymbol{v_s} = \boldsymbol{q}(\theta_s, \varphi_s)P(\theta_s, \varphi_s, \gamma_s, \eta_s)$, $\boldsymbol{v_i} = \boldsymbol{q}(\theta_i, \varphi_i)P(\theta_i, \varphi_i, \gamma_i, \eta_i)$ are the quaternion-valued steering vector associated with the desired signal and the interference, respectively, where $\boldsymbol{q}(\theta_\tau, \varphi_\tau) = [q_{-M}(\theta_\tau, \varphi_\tau), \cdots, q_M(\theta_\tau, \varphi_\tau)]^T$ ($\tau = s, i$) denotes the spatial phase factor vector of array.

Using the quaternion-valued measurement vector of an array $\boldsymbol{x}(n)$, the output of a beamformer is

$$y(n) = \mathbf{w}^{\Delta}\boldsymbol{x}(n) \tag{6}$$

http://dx.doi.org/10.5772/67859

where $\mathbf{w}$ is the quaternion-valued weight vector and the symbol $(.)^{\Delta}$ denotes the quaternion transposition-conjugation operator. Then, the QMVDR beamformer can be derived by solving the following constrained optimization problem [2]:

$$J(\mathbf{w}) = \min\{\mathbf{w}^{\Delta}\mathbf{R}_{x}\mathbf{w}\}; \textit{subject to } \mathbf{w}^{\Delta}\boldsymbol{v}_{s} = 1 \tag{7}$$

where $\mathbf{R}_{x} = E\{\boldsymbol{x}(n)\boldsymbol{x}^{\Delta}(n)\}$ is the covariance matrix of the measurement vector. By using Lagrange multipliers, the solution of Eq. (7) is obtained, i.e.,

$$J = \mathbf{w}^{\Delta}\mathbf{R}_{x}\mathbf{w} + \lambda\mathbf{w}^{\Delta}\boldsymbol{v}_{s} \tag{8}$$

where λ is a real number. Based on the quaternion-valued gradient operator defined in Ref. [11], the following gradients need to be calculated:

$$\frac{\partial J}{\partial \mathbf{w}^{\Delta}} = \mathbf{R}_{x}\mathbf{w} + \lambda\boldsymbol{v}_{s} \tag{9}$$

Let Eq. (9) is equal to zero, then

$$\mathbf{w} = -\lambda\mathbf{R}_{x}^{-1}\boldsymbol{v}_{s} \tag{10}$$

Since $\mathbf{w}^{\Delta}\boldsymbol{v}_{s} = -\lambda\boldsymbol{v}_{s}^{\Delta}\mathbf{R}_{x}^{-1}\boldsymbol{v}_{s} = 1$, we have,

$$\lambda = \frac{-1}{\boldsymbol{v}_{s}^{\Delta}\mathbf{R}_{x}^{-1}\boldsymbol{v}_{s}} \tag{11}$$

Substituting Eq. (11) into Eq. (10), the weight vector of the QMVDR beamformer can be written as

$$\mathbf{w} = \frac{\mathbf{R}_{x}^{-1}\boldsymbol{v}_{s}}{\boldsymbol{v}_{s}^{\Delta}\mathbf{R}_{x}^{-1}\boldsymbol{v}_{s}} \tag{12}$$

Substituting Eq. (12) into Eq. (6), the quaternion-valued output of the QMVDR beamformer is given by

$$y(n) = s_{s}(n) + \mathbf{w}^{\Delta}\boldsymbol{v}_{i}s_{i}(n) + \mathbf{w}^{\Delta}\boldsymbol{n}(n) \tag{13}$$

where $\mathbf{w}^{\Delta}\boldsymbol{v}_{s} = 1$. To a linear symmetric array with $2M$ two-component vector-sensors, the signal to interference-plus-noise ratio ($SINR$) of quaternion-valued output $y(n)$ can be written in the simple form (the proof is in Appendix 1 of Ref. [4])

$$SINR_{y} = \xi_{s}|P_{s}|^{2}\left(M - \frac{|P_{i}|^{2}|\boldsymbol{q}_{s}^{H}\boldsymbol{q}_{i}|^{2}}{4\xi_{i}^{-1} + 4M|P_{i}|^{2}}\right) \tag{14}$$

where the input signal-to-noise ratio (SNR) $\xi_{s} = \frac{\sigma_{s}^{2}}{\sigma_{n}^{2}}$ and the input interference-to-noise ratio (INR) $\xi_{i} = \frac{\sigma_{i}^{2}}{\sigma_{n}^{2}}$.

4. Interference and noise canceller (INC) based on QMVDR

Using the **C**-expansion of quaternions, $y(n)$ can be written as

$$y(n) = y_1(n) + j\, y_2(n) \tag{15}$$

where $y_1(n)$ and $y_2(n)$ are two complex-valued components of $y(n)$, i.e.,

$$y_1(n) = s_s(n) + (\mathbf{w}^{\Delta}\boldsymbol{v_i})_1 s_i(n) + (\mathbf{w}^{\Delta}\boldsymbol{n}(n))_1;\; y_2(n) = (\mathbf{w}^{\Delta}\boldsymbol{v_i})_2 s_i(n) + (\mathbf{w}^{\Delta}\boldsymbol{n}(n))_2 \tag{16}$$

$(.)_1$ and $(.)_2$ denote, respectively, first and second complex-valued components of a quaternion. The expansion (16) highlights the fact that $y_2(n)$ does not include the desired signal, but include only the interference and noise. By employing $y_2(n)$, we can partly cancel the interference and noise component in $y_1(n)$. Thus, an INC based on the QMVDR is shown in **Figure 2**.

The INC is a spatio-temporal processing, i.e., first part is a spatio filter and second part is a temporal filter. Then, the output of INC may be written as

$$\begin{aligned} y_s(n) &= y_1(n) - w_c^*\, y_2(n) \\ &= s_s(n) + ((\mathbf{w}^{\Delta}\boldsymbol{v_i})_1 - w_c^*(\mathbf{w}^{\Delta}\boldsymbol{v_i})_2) s_i(n) + ((\mathbf{w}^{\Delta}\boldsymbol{n}(n))_1 - w_c^*(\mathbf{w}^{\Delta}\boldsymbol{n}(n))_2) \\ &= s_s(n) + w_i s_i(n) + \varepsilon(n) \end{aligned} \tag{17}$$

where w_c is a complex weight, which can be given by the Wiener-Hoft equation

$$w_c = \frac{r_{y_2 y_1}}{R_{y_2}} \tag{18}$$

where $r_{y_2 y_1} = E\{y_2(n) y_1^*(n)\}$ and $R_{y_2} = E\{y_2(n) y_2^*(n)\}$. Following the proof given in Appendix 2 of Ref. [4], we have

$$w_c = \frac{(\mathbf{w}^{\Delta}\boldsymbol{v_i})_2 (\mathbf{w}^{\Delta}\boldsymbol{v_i})_1^* \xi_i}{|(\mathbf{w}^{\Delta}\boldsymbol{v_i})_2|^2 \xi_i + \|\mathbf{w}\|^2} \tag{19}$$

If ξ_i is very small, w_c is approximately equal to 0. Whereas, if ξ_i is very large, w_c is approximately equal to $\frac{(\mathbf{w}^{\Delta}\boldsymbol{v_i})_1^*}{(\mathbf{w}^{\Delta}\boldsymbol{v_i})_2^*}$. In this case, the interference can be cancelled. From Eq. (17), the *SINR* in the complex output $y_s(n)$ is given by

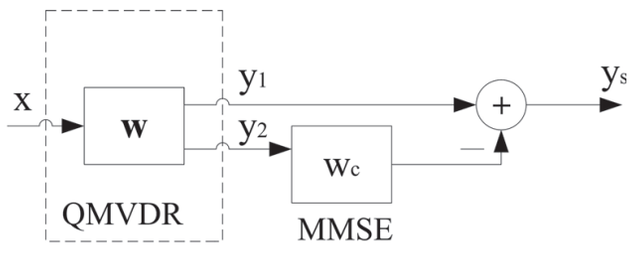

Figure 2. INC based on the QMVDR.

http://dx.doi.org/10.5772/67859

$$SINR_{y_s} = \frac{\xi_s}{\|\mathbf{w}\|^2}\left(1 - \frac{\sigma_i^2|(\mathbf{w}^{\Delta}\boldsymbol{v_i})_1|^2}{\sigma_n^2\|\mathbf{w}\|^2 + \sigma_i^2|\mathbf{w}^{\Delta}\boldsymbol{v_i}|^2}\right) = \kappa(1-\kappa_i) \tag{20}$$

where we define $\kappa = \frac{\xi_s}{\|\mathbf{w}\|^2}$ and $\kappa_i = \frac{\sigma_i^2|(\mathbf{w}^{\Delta}\boldsymbol{v_i})_1|^2}{\sigma_n^2\|\mathbf{w}\|^2+\sigma_i^2|\mathbf{w}^{\Delta}\boldsymbol{v_i}|^2}$. The proof is in Appendix 3 of Ref. [4]. Clearly, $SINR_{y_s}$ increases with an increase in κ but decreases with an increase in κ_i.

Next, we show the effect of sources parameters on κ and κ_i. Following the proof given in Appendix 4 of Ref. [4], we have

$$\kappa = \xi_s|P_s|^2\left(2M - \frac{|P_i|^2|\boldsymbol{q}_s^H\boldsymbol{q}_i|^2}{2\xi_i^{-1} + 2M|P_i|^2}\right)\frac{2M-\mu}{2M-\mu(1+\varepsilon)} = 2SINR_y\beta \tag{21}$$

where

$$\beta = \frac{2M-\mu}{2M-\mu(1+\varepsilon)};\ \mu = \frac{|P_i|^2|\boldsymbol{q}_s^H\boldsymbol{q}_i|^2}{2\xi_i^{-1} + 2M|P_i|^2};\ \varepsilon = \frac{\xi_i^{-1}}{\xi_i^{-1} + M|P_i|^2} \tag{22}$$

Obviously, the gain $\beta \geq 1$ because of $0 \leq \varepsilon < 1$. Then, $\kappa \geq 2SINR_y$.

From Eq. (21), κ depends mainly on separation between the DOAs of the desired signal and interference (i.e., $|\boldsymbol{q}_s^H\boldsymbol{q}_i|^2$). The dependencies of κ on $|\boldsymbol{q}_s^H\boldsymbol{q}_i|^2$ are shown in the following consequences:

1. When $\boldsymbol{q}_s = \boldsymbol{q}_i$ (no separation in DOA), $\mu = \frac{2|P_i|^2M^2}{\xi_i^{-1}+M|P_i|^2}$ because of $\boldsymbol{q}_s^H\boldsymbol{q}_i = 2M$. Then, $\beta = 1 + M\xi_i|P_i|^2$ and $\kappa = 2M\xi_i|P_i|^2$. In the case that M is constant, β increases with an increase in ξ_i and $|P_i|^2$, but κ increases with an increase in ξ_s and $|P_s|^2$.

2. When the separation between the DOAs of the desired signal and interference increases, $|\boldsymbol{q}_s^H\boldsymbol{q}_i|$ decreases. This results in the reduction of μ. Then, the both β and κ also reduce. When $\mu = \frac{2|P_i|^2M^2}{2\xi_i^{-1}+M|P_i|^2}$ (i.e., $|\boldsymbol{q}_s^H\boldsymbol{q}_i| = 2M\sqrt{\frac{1+M\xi_i|P_i|^2}{2+M\xi_i|P_i|^2}}$), $\kappa = 2M\xi_s|P_s|^2\left(\frac{4(1+M\xi_i|P_i|^2)}{(2+M\xi_i|P_i|^2)^2}\right)$ reaches to a minimum value. In this case, if $|\boldsymbol{q}_s^H\boldsymbol{q}_i| = \sqrt{2}M$ and $\kappa = 2M\xi_s|P_s|^2$. Along with an increase in ξ_i, the value of $|\boldsymbol{q}_s^H\boldsymbol{q}_i|$, which results in a minimum value of κ, tends to $2M$. Thus, the minimum value of κ tends to 0. Afterwards, κ will increase with a decrease in $|\boldsymbol{q}_s^H\boldsymbol{q}_i|$.

3. When $|\boldsymbol{q}_s^H\boldsymbol{q}_i| = 0$ (i.e., $\mu = 0$), $\beta = 1$ and $\kappa = 2M\xi_s|P_s|^2$. In this case, $\kappa = 2SINR_y$.

In addition, κ depends also on the input *INR* ξ_i, the array's element number $2M$ and the interference response $|P_i|^2$ and the desired signal response $|P_s|^2$.

In order to illustrate the previous discussions, **Figure 3(a)** and **(b)** displays, respectively, the variations of κ as a function of the desired signal's arrival angles θ_s and φ_s for several values of ξ_i, where $\theta_i = 90^\circ$ $\varphi_i = 60^\circ$; $\varphi_s = 60^\circ$ in **Figure 3(a)** and $\theta_s = 90^\circ$ in **Figure 3(b)**, where a linear symmetric antenna array is used with four (i.e., $M = 2$) two-component vector-sensor.

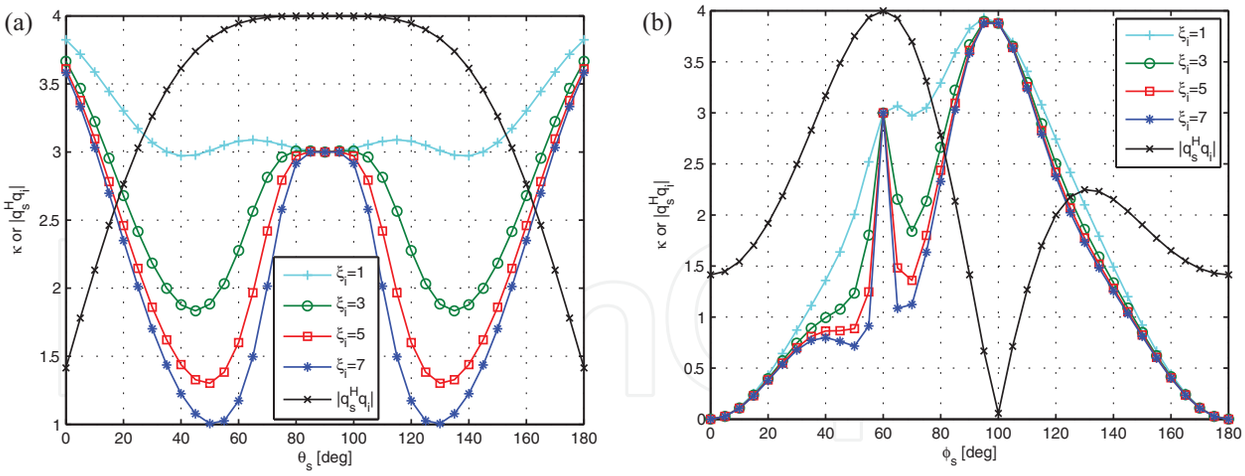

Figure 3. Variations of κ as a function of the desired signal's arrival angles θ_s and φ_s.

Each two-component vector-sensor has one electric dipole and one magnetic loop co-aligned along the x-axis, and four vector-sensors are spaced half a wavelength apart. It is assumed that the desired signal with ξ_s = 1 and the interference have the same polarization parameters ($\gamma_s = \gamma_i = 30^\circ, \eta_s = \eta_i = 30^\circ$). Simulation results in **Figure 3** are in agreement with the previous discussions. From **Figure 3(a)**, it is seen that $|\boldsymbol{q}_s^H \boldsymbol{q}_i| \approx 4$ and $\kappa \approx 3$ as $\theta_s \approx 90^\circ$. The cause of this phenomenon is that $|P_s|^2 = \sin^2\varphi_s + \cos^2\varphi_s \cos^2\theta_s$ for the two-component vector-sensor used in this example. When $\theta_s \approx 90^\circ$, $|P_s|^2 \approx 0.75$. In cases of $|\boldsymbol{q}_s^H \boldsymbol{q}_i| = 4$, $\kappa \approx 3$. Along θ_s is away from 90°, $|\boldsymbol{q}_s^H \boldsymbol{q}_i|$ decreases. This results in the reduction of κ. From **Figure 3(b)**, it is seen that $|\boldsymbol{q}_s^H \boldsymbol{q}_i| \approx 4$ and $\kappa \approx 3$ as $\varphi_s \approx 60^\circ$. This is as same as **Figure 3(a)**. In addition, it is noted that $|\boldsymbol{q}_s^H \boldsymbol{q}_i| \approx 0$ and $\kappa \approx 4$ as $\varphi_s \approx 100^\circ$. The cause of this phenomenon is that $|P_s|^2 \approx 1$ in cases of $\varphi_s \approx 100^\circ$ and $\kappa \approx 4$ in cases of $|\boldsymbol{q}_s^H \boldsymbol{q}_i| = 0$. When $\varphi_s = 0^\circ$ or $\varphi_s = 180^\circ$, $|P_s|^2 = 0$, then, $\kappa = 0$.

Since the output interference-plus-noise power $\mathbf{w}^\Delta \mathbf{R}_{in} \mathbf{w} = \sigma_n^2 \|\mathbf{w}\|^2 + \sigma_i^2 |\mathbf{w}^\Delta \boldsymbol{v}_i|^2$, we have

$$\kappa_i = \frac{\sigma_i^2 |(\mathbf{w}^\Delta \boldsymbol{v}_i)_1|^2}{\sigma_n^2 \|\mathbf{w}\|^2 + \sigma_i^2 |\mathbf{w}^\Delta \boldsymbol{v}_i|^2} = \frac{\sigma_i^2 |(\mathbf{w}^\Delta \boldsymbol{v}_i)_1|^2}{\mathbf{w}^\Delta \mathbf{R}_{in} \mathbf{w}} \tag{23}$$

where $0 \le \kappa_i \le 1$ because of $0 \le |(\mathbf{w}^\Delta \boldsymbol{v}_i)_1|^2 \le |\mathbf{w}^\Delta \boldsymbol{v}_i|^2$. Following the proof given in Appendix 1 of Ref. [4], κ_i is further written as

$$\kappa_i = \xi_i |P_s|^2 \left(M - \frac{|P_i|^2 |\boldsymbol{q}_s^H \boldsymbol{q}_i|^2}{4\xi_i^{-1} + 4M|P_i|^2} \right) |(\mathbf{w}^\Delta \boldsymbol{v}_i)_1|^2 \tag{24}$$

Obviously, κ_i = 0 at $|(\mathbf{w}^\Delta \boldsymbol{v}_i)_1| = 0$ or $\xi_i = 0$. And κ_i increases with an increase in $|(\mathbf{w}^\Delta \boldsymbol{v}_i)_1|^2$. In addition, κ_i depends also on the array's element number $2M$ and the interference response $|P_i|^2$.

http://dx.doi.org/10.5772/67859

Following the proof given in Appendix 5 of Ref. [4], we have

$$(\mathbf{w}^{\Delta}\boldsymbol{v_i})_1 = \alpha(\boldsymbol{v_s}^{\Delta}\boldsymbol{v_i})_1 = \alpha|\boldsymbol{q}_s^H\boldsymbol{q}_i|(P_s{}^*P_i)_1 \tag{25}$$

where

$$\alpha = \frac{\xi_i^{-1}}{|P_s|^2}\left(\frac{2}{4M\xi_i^{-1} + |P_i|^2(4M^2 - |\boldsymbol{q}_s^H\boldsymbol{q}_i|^2)}\right) \tag{26}$$

From Eqs. (25) and (26), $(\mathbf{w}^{\Delta}\boldsymbol{v_i})_1$ depends not only on the separation between the DOAs of the desired signal and interference (i.e., $|\boldsymbol{q}_s^H\boldsymbol{q}_i|$), but also on the difference between the polarizations of the desired signal and interference (i.e., $(P_s{}^*P_i)_1$). The dependencies of $(\mathbf{w}^{\Delta}\boldsymbol{v_i})_1$ and κ_i on $|\boldsymbol{q}_s^H\boldsymbol{q}_i|$ and $(P_s{}^*P_i)_1$) are shown in the following consequences:

1. When $\boldsymbol{q}_s = \boldsymbol{q}_i$ (i.e., no separation in DOA), $(\mathbf{w}^{\Delta}\boldsymbol{v_i})_1 = \frac{P_{s1}^* P_{i1} + P_{s2}^* P_{i2}}{|P_s|^2}$ because of $|\boldsymbol{q}_s^H\boldsymbol{q}_i| = 2M$. At the same time, if $P_s = P_i$ (i.e., no difference in polarization), $(\mathbf{w}^{\Delta}\boldsymbol{v_i})_1 = 1$ because of $P_{s1}^*P_{i1} + P_{s2}^*P_{i2} = |P_s|^2$ So, $\kappa_i = M\xi_i|P_s|^2\left(1 - \frac{M|P_i|^2}{\xi_i^{-1} + M|P_i|^2}\right)$ reaches to a maximum value. Whereas if the polarizations of the desired signal are an orthogonal with that of interference (i.e., $\gamma_s + \gamma_i = \frac{\pi}{2}$, $\eta_s - \eta_i = \pi$), $(\mathbf{w}^{\Delta}\boldsymbol{v_i})_1 = 0$ because of $(P_s{}^*P_i)_1 = 0$. So, κ_i reaches to a minimum value.

2. When the separation between the DOAs of the desired signal and interference increases, $|\boldsymbol{q}_s^H\boldsymbol{q}_i|$ decreases. This results in the reduction of $(\mathbf{w}^{\Delta}\boldsymbol{v_i})_1$. In addition, the increase in the difference between the polarizations of the desired signal and interference also results in the reduction of $(\mathbf{w}^{\Delta}\boldsymbol{v_i})_1$. Thus, κ_i reduces.

3. When $|\boldsymbol{q}_s^H\boldsymbol{q}_i| = 0$ or $(P_s{}^*P_i)_1 = 0$, $(\mathbf{w}^{\Delta}\boldsymbol{v_i})_1 = 0$. Thus, $\kappa_i = 0$. In the absence of the interference (i.e., $\xi_i = 0$), $\kappa_i = 0$.

Finally, we analyse the performance of the INC. From Eq. (20) and above analysis, we can obtain the following consequences:

1. When $|\boldsymbol{q}_s^H\boldsymbol{q}_i| = 0$, $\kappa = 2M\xi_s|P_s|^2$ and $\kappa_i = 0$. This implies that the separation between the DOA's of the desired signal and interference reaches to maximum. In this case, we can obtain the maximum value of $SINR_{y_s}$, i.e., $SINR_{y_s\max} = 2M\xi_s|P_s|^2$. Further, $|\boldsymbol{q}_s^H\boldsymbol{q}_i|$ increases with a decrease in the separation in DOA. Thus, $SINR_{y_s}$ will reduce due to the decrease in κ and the increase in κ_i. When $|\boldsymbol{q}_s^H\boldsymbol{q}_i| = 2M\sqrt{\frac{1+M\xi_i|P_i|^2}{2+M\xi_i|P_i|^2}}$), κ reaches to a minimum value. In this case, we can obtain the minimum value of $SINR_{y_s}$ if κ_i reaches to a maximum value.

2. When $(P_s{}^*P_i)_1 = 0$, $\kappa_i = 0$. In this case, we can obtain the maximum value of $SINR_{y_s}$, i.e., $SINR_{y_s\max} = 2M\xi_s|P_s|^2$, if $|\boldsymbol{q}_s^H\boldsymbol{q}_i| = 2M$. This implies that even though no separation between the DOAs of the desired signal and interference, $SINR_{y_s}$ can reach to maximum by using the orthogonally between the polarizations of the desired signal and interference.

Further, $|(P_s{}^*P_i)_1|$ increases with a decrease in the difference in polarizations. Thus, $SINR_{y_s}$ will reduce due to the increase in κ_i.

3. When $\xi_i = 0$ (i.e., in the absence of interference), $\kappa = 2M\xi_s|P_s|^2$ and $\kappa_i = 0$. In this case, we can obtain the maximum value of $SINR_{y_s}$, i.e., $SINR_{y_s\max} = 2M\xi_s|P_s|^2$. Further, $SINR_{y_s}$ decreases with an increase in ξ_i. In the presence of a strong interference (i.e., $\xi_i^{-1} \approx 0$), $SINR_{y_s}$ can be approximated as

$$\mathrm{SINR}_{y_s} \approx \xi_s|P_s|^2\left(2M - \frac{|\boldsymbol{q}_s^H\boldsymbol{q}_i|^2}{2M}\right)\left(1 - \frac{|(\boldsymbol{v_s}^{\Delta}\boldsymbol{v_i})_1|^2}{|\boldsymbol{v_s}^{\Delta}\boldsymbol{v_i}|^2}\right) \tag{27}$$

where $\kappa \approx \xi_s|P_s|^2\left(2M - \frac{|\boldsymbol{q}_s^H\boldsymbol{q}_i|^2}{2M}\right)$ and $\kappa_i = \frac{|(\boldsymbol{v_s}^{\Delta}\boldsymbol{v_i})_1|^2}{|\boldsymbol{v_s}^{\Delta}\boldsymbol{v_i}|^2}$. Expression (27) highlights the fact that in the presence of a strong interference, $SINR_{y_s} \approx 0$ in the case of no separation between the DOAs of the desired signal and interference (i.e., $\boldsymbol{q}_s = \boldsymbol{q}_i$) or no difference between the polarizations of the desired signal and interference (i.e., $P_s = P_i$). This implies that the INC fails.

4. When the vector-sensor number $2M$ in array increases, κ increases and κ_i decreases. Thus, $SINR_{y_s}$ is an increasing function of $2M$. Since κ increases with an increase in $|P_s|^2$, but κ_i decreases with an increase in $|P_s|^2$, $SINR_{y_s}$ is an increasing function of $|P_s|^2$. Further, $SINR_{y_s}$ is a decreasing function of $|P_i|^2$ because κ decreases with an increase in $|P_i|^2$.

5. The quaternion semi-widely linear (QSWL) beamformer

According to the definition in Ref. [12], the involution of a quaternion x over a pure unit quaternion i is $x^{(i)} = ixi^{-1} = ixi^* = -ixi$ and it represents the reflection of x over the plane spanned by $\{1, i\}$. A quaternion vector $\boldsymbol{x}$ is C^i-proper iff it can be represented by means of two jointly proper complex vectors in the plane spanned by $\{1, i\}$. The augmented covariance matrix of a C^i-proper quaternion vector $\boldsymbol{x}$ can be written as

$$\mathbf{R}_{\overline{x},\,\overline{x}} = \mathrm{E}\{\overline{\boldsymbol{x}}\,\overline{\boldsymbol{x}}^{\Delta}\} = \begin{bmatrix} \mathbf{R}_{\tilde{\boldsymbol{x}},\tilde{\boldsymbol{x}}} & 0 \\ 0 & \mathbf{R}_{\tilde{\boldsymbol{x}},\tilde{\boldsymbol{x}}^j} \end{bmatrix} \tag{28}$$

where $\overline{\boldsymbol{x}} = [\boldsymbol{x}^T, \boldsymbol{x}^{(i)T}, \boldsymbol{x}^{(j)T}, \boldsymbol{x}^{(k)T}]^T$ is the augmented quaternion vector; $\tilde{\boldsymbol{x}} = [\boldsymbol{x}^T, \boldsymbol{x}^{(i)T}]^T$ is the semi-augmented quaternion vector and $\mathbf{R}_{\tilde{\boldsymbol{x}},\tilde{\boldsymbol{x}}} = \mathrm{E}\{\tilde{\boldsymbol{x}}\,\tilde{\boldsymbol{x}}^{\Delta}\}$ is the semi-augmented covariance matrix of quaternion vector $\boldsymbol{x}$. In comparison with the semi-augmented covariance matrix $\mathbf{R}_{\tilde{\boldsymbol{x}},\tilde{\boldsymbol{x}}}$, the augmented covariance matrix $\mathbf{R}_{\overline{\boldsymbol{x}},\overline{\boldsymbol{x}}}$ has not more extra information. In other words, the *full-widely* linear processing is equivalent to the *semi-widely* linear processing in handling the C^i-proper quaternion vector. We should not expect that the performance is improved by replacing *semi-widely* linear processing with *full-widely* linear processing.

The most general linear processing is *full-widely* linear processing, which consists in the simultaneous operation on the quaternion vector and its three involutions. Then, a quaternion widely linear beamformer can be written as

$$y(n) = \mathbf{w}^{\Delta}\boldsymbol{x}(n) + \ \mathbf{G}^{\Delta}\boldsymbol{x}^{(i)}(n) + \mathbf{H}^{\Delta}\boldsymbol{x}^{(j)}(n) + \mathbf{F}^{\Delta}\boldsymbol{x}^{(k)}(n) \tag{29}$$

where **W, G, H** and **F** denote the quaternion-valued weight vectors. $\boldsymbol{x}^{(i)}(n)$, $\boldsymbol{x}^{(j)}(n)$ and $\boldsymbol{x}^{(k)}(n)$ denote the quaternion involution of $\boldsymbol{x}(n)$ over a pure unit imaginary i, j and k, respectively.

The *full-widely* linear processing is optimal processing for the Q-improper quaternion vector. Since the quaternion-valued vector $\boldsymbol{x}(n)$ is C^i-proper vector, however, the optimal processing reduces to *semi-widely* linear processing. Because the *semi-widely* linear processing consists only in the simultaneous operation on the quaternion vector and its involution over i, the general expression of a quaternion *semi-widely* linear (QSWL) beamformer can be written as Ref. [5]

$$y(n) = \mathbf{W}^{\Delta}\boldsymbol{x}(n) + \ \mathbf{G}^{\Delta}\boldsymbol{x}^{(i)}(n) \tag{30}$$

where $\boldsymbol{x}^{(i)}(n)$ is given by

$$\boldsymbol{x}^{(i)}(n) = -i\boldsymbol{x}(n)i = \boldsymbol{v_s}^{(i)}s_s(n) + v_{\boldsymbol{i}}{}^{(i)}s_i(n) + \boldsymbol{n}^{(i)}(n) \tag{31}$$

Moreover, we can write the quaternion-valued output series $y(n)$ in the following *Cayley-Dickson* representation

$$y(n) = ((\mathbf{W}^{\Delta}\boldsymbol{x}(n))_1 + (\mathbf{G}^{\Delta}\boldsymbol{x}^{(i)}(n))_1) + j((\mathbf{W}^{\Delta}\boldsymbol{x}(n))_2 + (\mathbf{G}^{\Delta}\boldsymbol{x}^{(i)}(n))_2) = y_1(n) + jy_2(n) \tag{32}$$

where y_1 and y_2 denote, respectively, first and second complex-valued components of a quaternion y. Thus, the QSWL beamformer has two complex-valued output series $y_1(n)$ and $y_2(n)$ in the planes spanned by {1, i}, where $y_1(n) = (\mathbf{W}^{\Delta}\boldsymbol{x}(n))_1 + (\mathbf{G}^{\Delta}\boldsymbol{x}^{(i)}(n))_1)$ and $y_2(n) = (\mathbf{W}^{\Delta}\boldsymbol{x}(n))_2 + (\mathbf{G}^{\Delta}\boldsymbol{x}^{(i)}(n))_2)$. Since the complex 'long vector' beamformers have only one complex-valued output series $y_1(n)$, the QSWL beamformer can obtain more information than the conventional 'long vector' beamformer. The increase of information results in the improvement of QSWL beamformer's performance. In addition, we incorporate both the information on $\boldsymbol{x}(n)$ and $\boldsymbol{x}^{(i)}(n)$, so that the QSWL beamformer with different characteristics may be obtained by designing two weight vectors **W** and **G** under some different criterions.

6. The QSWL generalized sidelobe canceller

In this section, a useful implementation of the QSWL beamformer, i.e., QSWL generalized sidelobe sanceller (GSC), is proposed. The QSWL GSC, which is depicted in **Figure 4**, consists of two-stage beamformers. In first-stage beamformer (weight vector is **W**), we attempt to extract a desired signal without any distortion from observed data. To cancel interferences, we attempt to estimate interferences in second-stage beamformer (weight vector is **G**). By

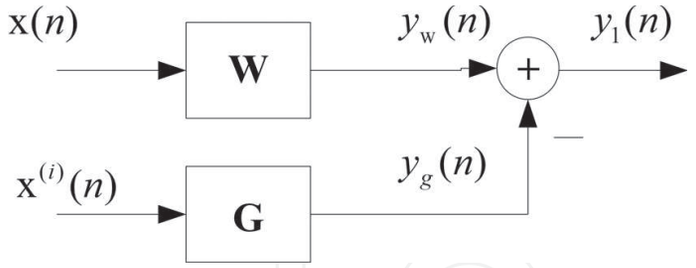

Figure 4. The structure of QSWL GSC.

employing the output of second-stage beamformer to cancel interferences in the output of first-stage beamformer, there is no interference in the output of the QSWL GSC. Compared with the complex 'long vector' beamformers, the advantages of two-stage beamformers are that the main beam can always point to desired signal's direction, even if the separation between the DOAs of the desired signal and interference is less, and the robustness to DOA mismatch is improved.

In the following, we derive the expressions of quaternion-valued weight vectors **W** in first-stage beamformer and **G** in second-stage beamformer. Because the quaternion-valued output $y(n)$ has two complex-valued components in the planes spanned by {1, i}, i.e., $y_1(n)$ and $y_2(n)$, we define the first complex-valued output component as the output of the QSWL GSC. Thus, the complex-valued output of the QSWL GSC is written as

$$y_{\mathrm{GSC}}(n) = (y(n))_1 = y_w(n) - y_g(n) \tag{33}$$

where $y_w(n)$ is the complex-valued output of the first-stage beamformer, i.e., $y_w(n) = (\mathbf{W}^{\Delta}\boldsymbol{x}(n))_1$; $y_g(n)$ is the complex-valued output of the second-stage beamformer, i.e., $y_g(n) = (\mathbf{G}^{\Delta}\boldsymbol{x}^{(i)}(n))_1$

6.1. The first-stage beamformer

From Eq. (5), we have

$$y_w(n) = (\mathbf{W}^{\Delta}\boldsymbol{v_s})_1 s_s(n) + (\mathbf{W}^{\Delta}\boldsymbol{v_i})_1 s_i(n) + (\mathbf{W}^{\Delta}\boldsymbol{n}(n))_1 \tag{34}$$

In the first-stage beamformer, we attempt to minimize the interference-plus-noise energy in $y_w(n)$, subject to the constraint $(\mathbf{w}^{\Delta}\boldsymbol{v_s})_1 = 1$.

Since the *Cayley-Dickson* representations of **W**, $\boldsymbol{v_s}$, $\boldsymbol{v_i}$ and $\boldsymbol{n}(n)$ are, respectively, $\mathbf{W} = \mathbf{W}_1 + \mathrm{j}\,\mathbf{W}_2$, $\boldsymbol{v_s} = \boldsymbol{v_{s1}} + j\,\boldsymbol{v_{s2}}$, $\boldsymbol{v_i} = \boldsymbol{v_{i1}} + j\,\boldsymbol{v_{i2}}$ and $\boldsymbol{n}(n) = \boldsymbol{n}_1(n) + j\,\boldsymbol{n}_2(n)$, we have

$$(\mathbf{W}^{\Delta}\boldsymbol{v_s})_1 = \mathbf{W}_1^H\boldsymbol{v_{s1}} + \mathbf{W}_2^H\boldsymbol{v_{s2}} = \overline{\mathbf{W}}^H\overline{\mathbf{V}}_s \tag{35}$$

$$(\mathbf{W}^{\Delta}\boldsymbol{v_i})_1 = \mathbf{W}_1^H\boldsymbol{v_{i1}} + \mathbf{W}_2^H\boldsymbol{v_{i2}} = \overline{\mathbf{W}}^H\overline{\mathbf{V}}_i \tag{36}$$

$$(\mathbf{W}^{\Delta}\boldsymbol{n}(n))_1 = \mathbf{W}_1^H\boldsymbol{n}_1(n) + \mathbf{W}_2^H\boldsymbol{n}_2(n) = \overline{\mathbf{W}}^H\overline{\mathbf{N}}(n) \tag{37}$$

http://dx.doi.org/10.5772/67859

where $\overline{\mathbf{W}} = \begin{bmatrix} \mathbf{W}_1 \\ \mathbf{W}_2 \end{bmatrix}$, $\overline{\mathbf{V}}_s = \begin{bmatrix} \boldsymbol{v}_{s1} \\ \boldsymbol{v}_{s2} \end{bmatrix}$, $\overline{\mathbf{V}}_i = \begin{bmatrix} \boldsymbol{v}_{i1} \\ \boldsymbol{v}_{i2} \end{bmatrix}$, $\overline{\mathbf{N}}(n) = \begin{bmatrix} \boldsymbol{n}_1(n) \\ \boldsymbol{n}_2(n) \end{bmatrix}$. Superscript $(.)^H$ denotes the complex conjugate and transpose operator. Thus, Eq. (34) can be rewritten as

$$y_w(n) = \overline{\mathbf{W}}^H \overline{\mathbf{V}}_s s_s(n) + \overline{\mathbf{W}}^H \overline{\mathbf{V}}_i \, s_i(n) + \overline{\mathbf{W}}^H \overline{\mathbf{N}}(n) \tag{38}$$

Then, $\overline{\mathbf{W}}$ can be derived by solving the following constrained optimization problem:

$$J(\overline{\mathbf{W}}) = \min\{\overline{\mathbf{W}}^H \mathbf{R}_{in} \overline{\mathbf{W}}\}; \; subject \; to \; \overline{\mathbf{W}}^H \overline{\mathbf{V}}_s = 1 \tag{39}$$

where

$$\mathbf{R}_{in} = \begin{bmatrix} \mathrm{E}\{(\boldsymbol{x}_{in}(n))_1 \, (\boldsymbol{x}_{in}(n))_1^H\} & \mathrm{E}\{(\boldsymbol{x}_{in}(n))_1 \, (\boldsymbol{x}_{in}(n))_2^H\} \\ \mathrm{E}\{(\boldsymbol{x}_{in}(n))_2 \, (\boldsymbol{x}_{in}(n))_1^H\} & \mathrm{E}\{(\boldsymbol{x}_{in}(n))_2 \, (\boldsymbol{x}_{in}(n))_2^H\} \end{bmatrix} \tag{40}$$

is the covariance matrix and $\boldsymbol{x}_{in}(n) = \boldsymbol{v}_i s_i(n) + \boldsymbol{n}(n)$ is the measurement vector of array in the absence of the desired signal. The solution of this constrained optimization problem is obtained by using Lagrange multipliers, that is

$$\overline{\mathbf{W}} = \frac{\mathbf{R}_{in}^{-1} \, \overline{\mathbf{V}}_s}{\overline{\mathbf{V}}_s^H \mathbf{R}_{in}^{-1} \, \overline{\mathbf{V}}_s} \tag{41}$$

If the interferences are uncorrelated with the additive noise, $\overline{\mathbf{W}}$ can be written in the simple form (the proof is in Appendix A of Ref. [5])

$$\overline{\mathbf{W}} = \frac{\varepsilon \overline{\mathbf{V}}_s - (P_i{}^{\Delta} P_s)_1 \boldsymbol{q}_i^H \boldsymbol{q}_s \overline{\mathbf{V}}_i}{\mu} \tag{42}$$

where

$$\mu = 2M|P_s|^2 \varepsilon - |(P_i{}^{\Delta} P_s)_1|^2 |\boldsymbol{q}_i^H \boldsymbol{q}_s|^2 \; ; \; \varepsilon = \xi_i^{-1} + \; 2M|P_i|^2 \tag{43}$$

where ξ_i denotes the input interference-to-noise ratio (INR). Moreover, the quaternion-valued optimal weight vector $\mathbf{W}_o$ may be given by

$$\mathbf{W}_o = \boldsymbol{J}_1 \, \overline{\mathbf{W}} + j \, \boldsymbol{J}_2 \, \overline{\mathbf{W}} \tag{44}$$

where $\boldsymbol{J}_1 = [\mathbf{I}_{2M \times 2M}, \; \mathbf{0}_{2M \times 2M}]$ and $\boldsymbol{J}_2 = [\mathbf{0}_{2M \times 2M}, \; \mathbf{I}_{2M \times 2M}]$ are two selection matrices. It is noted that in some applications, such as Radar, $\mathbf{R}_{in}$ may be estimated in intervals of no transmitted signal. But, $\mathbf{R}_{in}$ is not obtained in other applications, such as Communications. In these applications, we may replace $\mathbf{R}_{in}$ by $\mathbf{R}_x$, where

$$\mathbf{R}_x = \begin{bmatrix} \mathrm{E}\{(\boldsymbol{x}(n))_1 \, (\boldsymbol{x}(n))_1^H\} & \mathrm{E}\{(\boldsymbol{x}(n))_1 \, (\boldsymbol{x}(n))_2^H\} \\ \mathrm{E}\{(\boldsymbol{x}(n))_2 \, (\boldsymbol{x}(n))_1^H\} & \mathrm{E}\{(\boldsymbol{x}(n))_2 \, (\boldsymbol{x}(n))_2^H\} \end{bmatrix} \tag{45}$$

is the covariance matrix and $\mathbf{x}(n)$. When the distortionless constraint is perfectly matched with the desired signal, the weight vector $\mathbf{W}_o$ is identical in both $\mathbf{R}_{in}$ and $\mathbf{R}_x$.

By using the optimal weight vector $\mathbf{W}_o$, the complex output of first-stage beamformer can be given by

$$y_w(n) = s_s(n) + (\mathbf{W}_o{}^{\Delta}\boldsymbol{v_i})_1\ s_i(n) + (\mathbf{W}_o{}^{\Delta}\boldsymbol{n}(n))_1 \tag{46}$$

6.2. The second-stage beamformer

From Eq. (31), we have

$$y_g(n) = (\mathbf{G}^{\Delta}\boldsymbol{v}_s^{(i)})_1 S_s(n) + (\mathbf{G}^{\Delta}\boldsymbol{v}_i^{(i)})_1\ S_i(n) + (\mathbf{G}^{\Delta}\boldsymbol{n}^{(i)}(n))_1 \tag{47}$$

In the second-stage beamformer, we attempt to minimize the noise energy in $y_g(n)$, subject to the constraints $(\mathbf{G}^{\Delta}\boldsymbol{v}_S^{(i)})_1 = 0$ and $(\mathbf{G}^{\Delta}\boldsymbol{v}_i^{(i)})_1 = (\mathbf{W}_o^{\Delta}\boldsymbol{v_i})_1$. In the following, two schemes are presented to implement this aim.

6.2.1 The Scheme 1, i.e., combined QPMC and MVDR

Let $= \mathbf{w}_{qs}\mathbf{w}_{MV}$, where $\mathbf{w}_{qs}$ is a quaternion-valued diagonal weight matrix and $\mathbf{w}_{MV}$ is a complex weight vector. In this scheme, the first is to achieve the constraint $(\mathbf{G}^{\Delta}\boldsymbol{v}_s^{(i)})_1 = 0$ by designing $\mathbf{w}_{qs}$, which is referred to quaternion polarization matched cancellation (QPMC); the second is to minimize the noise energy in $y_g(n)$ subject to the constraint $(\mathbf{G}^{\Delta}\boldsymbol{v}_i^{(i)})_1 = (\mathbf{W}_o^{\Delta}\boldsymbol{v_i})_1$ by designing $\mathbf{w}_{MV}$, which is referred to MVDR.

Let $\mathbf{w}_{qs} = \text{diag}\ \{\text{w}_{qs}(-M),\ \cdots, \text{w}_{qs}(M)\};$ then we have

$$\mathbf{G}^{\Delta}\boldsymbol{v}_s^{(i)} = \mathbf{w}_{MV}{}^H\mathbf{w}_{qs}^{\Delta}\boldsymbol{v}_s^{(i)} = \mathbf{w}_{MV}{}^H\begin{bmatrix} \text{w}_{qs}{}^*(-M)q_{-M}(\theta_s,\ \varphi_s)P_s^{(i)} \\ \vdots \\ \text{w}_{qs}{}^*(M)q_M(\theta_s,\ \varphi_s)P_s^{(i)} \end{bmatrix} \tag{48}$$

where superscript (.)* denotes the quaternion conjugate operator. From Eq. (48) and the constraint $(\mathbf{G}^{\Delta}\boldsymbol{v}_s^{(i)})_1 = 0$, we have the constraint $(\text{w}_{qs}{}^*(m)q_m(\theta_s,\ \varphi_s)P_s^{(i)})_1 = 0$, where $m = \{-M,\ \cdots, M\}$. When $\text{w}_{qs}(m) = q_m(\theta_s,\ \varphi_s)\ (a_{s2}^* + j\ a_{s1}^*)$, this constraint is satisfied. Thus, we can obtain

$$\mathbf{w}_{qs} = \text{diag}\ \{\boldsymbol{q_s}\}\ (a_{s2}^* + j\ a_{s1}^*) \tag{49}$$

where $\text{diag}\ \{\boldsymbol{q_s}\} = \text{diag}\ \{q_{-M}(\theta_s,\ \varphi_s), \cdots, q_M(\theta_s,\ \varphi_s)\}$. In the constraint $(\mathbf{G}^{\Delta}\boldsymbol{v}_s^{(i)})_1 = 0$, we insert $\mathbf{G} = \mathbf{w}_{qs}\mathbf{w}_{MV}$ into (47). Thus, $y_g(n)$ can be rewritten as

$$y_g(n) = \mathbf{w}_{MV}{}^H(\mathbf{w}_{qs}^{\Delta}\boldsymbol{v}_i^{(i)})_1\ s_i(n) + \mathbf{w}_{MV}{}^H(\mathbf{w}_{qs}^{\Delta}\boldsymbol{n}^{(i)}(n))_1 \tag{50}$$

Then, $\mathbf{w}_{MV}$ can be derived by solving the following constrained optimization problem:

http://dx.doi.org/10.5772/67859

$$J(\mathbf{w}_{MV}) = \min\{\mathbf{w}_{MV}{}^{H}\mathbf{R}_{qs}\mathbf{w}_{MV}\};\ \textit{subject to}\ \mathbf{w}_{MV}{}^{H}\ \tilde{\boldsymbol{V}}_{\boldsymbol{i}} = \overline{\mathbf{W}}^{H}\overline{\mathbf{V}}_{\boldsymbol{i}} \tag{51}$$

where $\mathbf{R}_{qs} = \mathrm{E}\{(\mathbf{w}_{qs}^{\Delta}\boldsymbol{x}^{(i)}(n))_1\ \left(\mathbf{w}_{qs}^{\Delta}\boldsymbol{x}^{(i)}(n)\right)_1^{H}\}$ is the covariance matrix and $\tilde{\boldsymbol{V}}_{\boldsymbol{i}} = (\mathbf{w}_{qs}^{\Delta}\boldsymbol{v}_{\boldsymbol{i}}^{(\boldsymbol{i})})_1$. The solution of this constrained optimization problem is obtained by using Lagrange multipliers, i.e.,

$$\mathbf{w}_{MV} = \frac{\mathbf{R}_{qs}^{-1}\ \tilde{\boldsymbol{V}}_{\boldsymbol{i}}}{\tilde{\boldsymbol{V}}_{\boldsymbol{i}}{}^{H}\mathbf{R}_{qs}^{-1}\tilde{\boldsymbol{V}}_{\boldsymbol{i}}}\overline{\mathbf{V}}_{\boldsymbol{i}}{}^{H}\overline{\mathbf{W}} \tag{52}$$

If the desired signal and interference are uncorrelated with the additive noise, $\mathbf{w}_{MV}$ can be written in the simple form (the proof is in Appendix B of Ref. [5])

$$\mathbf{w}_{MV} = \frac{\boldsymbol{g}_1}{\kappa}\tilde{\boldsymbol{V}}_{\boldsymbol{i}} \tag{53}$$

where

$$\kappa = \tilde{\boldsymbol{V}}_{\boldsymbol{i}}{}^{H}\tilde{\boldsymbol{V}}_{\boldsymbol{i}} = 2M(|a_{s2}|^2|a_{i1}|^2 + |a_{s1}|^2|a_{i2}|^2) - 2\mathcal{R}(a_{s1}a_{s2}^{*}a_{i2}a_{i1}^{*}(\boldsymbol{q}_{\boldsymbol{i}}{}^2)^{H}\boldsymbol{q}_{\boldsymbol{s}}{}^2) \tag{54}$$

$$g_1 = (\overline{\mathbf{W}}^{H}\overline{\mathbf{V}}_i)^{H} = \frac{\xi_i^{-1}(P_i{}^{\Delta}P_s)_1\boldsymbol{q}_i^{H}\boldsymbol{q}_s}{\mu} \tag{55}$$

where $\mathcal{R}$ (.) denotes the real part of a complex number. μ is given by Eq. (43).

6.2.2. The scheme 2, i.e. Linearly constrained minimum variance (LCMV) beamformer

In this scheme, we employ the LCMV beamformer as the second-stage beamformer. Since the *Cayley-Dickson* representations of $\mathbf{G}$, $\boldsymbol{v}_{\boldsymbol{s}}^{(\boldsymbol{i})}$, $\boldsymbol{v}_{\boldsymbol{i}}^{(\boldsymbol{i})}$ and $\boldsymbol{n}^{(i)}(n)$ are, respectively, $\mathbf{G} = \mathbf{G}_1 + j\,\mathbf{G}_2$, $\boldsymbol{v}_{\boldsymbol{s}}^{(\boldsymbol{i})} = \boldsymbol{v}_{s1} - j\boldsymbol{v}_{s2}$, $\boldsymbol{v}_{\boldsymbol{i}}^{(\boldsymbol{i})} = \boldsymbol{v}_{i1} - j\ \boldsymbol{v}_{i2}$ and $\boldsymbol{n}^{(i)}(n) = \boldsymbol{n}_1(n) - j\ \boldsymbol{n}_2(n)$, we have

$$(\mathbf{G}^{\Delta}\boldsymbol{v}_{\boldsymbol{s}}^{(\boldsymbol{i})})_1 = \mathbf{G}_1^{H}\boldsymbol{v}_{s1} - \mathbf{G}_2^{H}\boldsymbol{v}_{s2} = \overline{\mathbf{G}}^{H}\overline{\mathbf{V}}_{\boldsymbol{s}}^{(\boldsymbol{i})} \tag{56}$$

$$(\mathbf{G}^{\Delta}\boldsymbol{v}_{\boldsymbol{i}}^{(\boldsymbol{i})})_1 = \mathbf{G}_1^{H}\boldsymbol{v}_{i1} - \ \mathbf{G}_2^{H}\boldsymbol{v}_{i2} = \overline{\mathbf{G}}^{H}\overline{\mathbf{V}}_{\boldsymbol{i}}^{(\boldsymbol{i})} \tag{57}$$

$$(\mathbf{G}^{\Delta}\boldsymbol{n}^{(\boldsymbol{i})}(n))_1 = \mathbf{G}_1^{H}\boldsymbol{n}_1(n) - \ \mathbf{G}_2^{H}\boldsymbol{n}_2(n) = \overline{\mathbf{G}}^{H}\overline{\mathbf{N}}^{(\boldsymbol{i})}(n) \tag{58}$$

where $\overline{\mathbf{G}} = \begin{bmatrix}\mathbf{G}_1\\ \mathbf{G}_2\end{bmatrix}$; $\overline{\mathbf{V}}_{\boldsymbol{s}}^{(\boldsymbol{i})} = \begin{bmatrix}\boldsymbol{v}_{s1}\\ -\boldsymbol{v}_{s2}\end{bmatrix}$; $\overline{\mathbf{V}}_{\boldsymbol{i}}^{(\boldsymbol{i})} = \begin{bmatrix}\boldsymbol{v}_{i1}\\ -\boldsymbol{v}_{i2}\end{bmatrix}$; $\overline{\mathbf{N}}^{(\boldsymbol{i})}(n) = \begin{bmatrix}\boldsymbol{n}_1(n)\\ -\boldsymbol{n}_2(n)\end{bmatrix}$

Thus, Eq. (47) can be rewritten as

$$y_g(n) = \overline{\mathbf{G}}^{H}\overline{\mathbf{V}}_{\boldsymbol{s}}^{(\boldsymbol{i})}s_s(n) + \overline{\mathbf{G}}^{H}\overline{\mathbf{V}}_{\boldsymbol{i}}^{(\boldsymbol{i})}\ s_i(n) + \overline{\mathbf{G}}^{H}\overline{\mathbf{N}}^{(\boldsymbol{i})}(n) \tag{59}$$

Then, $\overline{\mathbf{G}}$ can be derived by solving the following constrained optimization problem:

$$J(\overline{\mathbf{G}}) = \min\{\overline{\mathbf{G}}^H \mathbf{R}_{inG} \overline{\mathbf{G}}\}; \textit{subject to } \overline{\mathbf{G}}^H \mathbf{C} = \mathbf{g}^H \tag{60}$$

where

$$\mathbf{R}_{inG} = \begin{bmatrix} \mathrm{E}\{(\boldsymbol{x}_{in}^{(i)}(n))_1 \, (\boldsymbol{x}_{in}^{(i)}(n))_1^H\} & \mathrm{E}\{(\boldsymbol{x}_{in}^{(i)}(n))_1 \, (\boldsymbol{x}_{in}^{(i)}(n))_2^H\} \\ \mathrm{E}\{(\boldsymbol{x}_{in}^{(i)}(n))_2 \, (\boldsymbol{x}_{in}^{(i)}(n))_1^H\} & \mathrm{E}\{(\boldsymbol{x}_{in}^{(i)}(n))_2 \, (\boldsymbol{x}_{in}^{(i)}(n))_2^H\} \end{bmatrix} \tag{61}$$

is the covariance matrix and $\boldsymbol{x}_{in}^{(i)}(n) = \boldsymbol{v}_i^{(i)} s_i(n) + \boldsymbol{n}^{(i)}(n)$ is the quaternion involution of $\boldsymbol{x}_{in}(n)$. $\mathbf{C} = [\overline{\mathbf{V}}_i^{(i)}, \overline{\mathbf{V}}_s^{(i)}]$ and $\mathbf{g}^H = [g_1^H, \, 0]$, where g_1 is given by Eq. (55). The solution of Eq. (60) is given by Van Trees [13]

$$\overline{\mathbf{G}} = \mathbf{R}_{inG}^{-1} \mathbf{C} (\mathbf{C}^H \mathbf{R}_{inG}^{-1} \mathbf{C})^{-1} \mathbf{g} \tag{62}$$

If the desired signal and interference are uncorrelated with the additive noise, $\overline{\mathbf{G}}$ can be written in the simple form (the proof is in Appendix C of Ref. [5])

$$\overline{\mathbf{G}} = \frac{g_1}{\nu} (2M|P_s|^2 \overline{\mathbf{V}}_i^{(i)} - (P_s{}^{\Delta} P_i)_1 \boldsymbol{q}_s^H \boldsymbol{q}_i \overline{\mathbf{V}}_s^{(i)}) \tag{63}$$

where

$$\nu = (2M)^2 |P_s|^2 |P_i|^2 - |(P_i{}^{\Delta} P_s)_1|^2 |\boldsymbol{q}_i^H \boldsymbol{q}_s|^2 = \mu - 2M\xi_i^{-1} |P_s|^2 \tag{64}$$

μ is given by (43). Moreover, the quaternion-valued optimal weight vector $\mathbf{G}_o$ may be given by

$$\mathbf{G}_o = \boldsymbol{J}_1 \, \overline{\mathbf{G}} + j \, \boldsymbol{J}_2 \, \overline{\mathbf{G}} \tag{65}$$

where $\boldsymbol{J}_1 = [\mathbf{I}_{2M\times 2M}, \; \mathbf{0}_{2M\times 2M}]$ and $\boldsymbol{J}_2 = [\mathbf{0}_{2M\times 2M}, \; \mathbf{I}_{2M\times 2M}]$ are two selection matrices.

By using the optimal weight vector $\mathbf{G}_o$, the complex output of second-stage beamformer can be given by

$$y_g(n) = (\mathbf{W}_o{}^{\Delta} \boldsymbol{v}_i)_1 \, s_i(n) + (\mathbf{G}_o{}^{\Delta} \boldsymbol{n}^{(i)}(n))_1 \tag{66}$$

Thus, the complex output of QSWL GSC may be rewritten as

$$y_{GSC}(n) = y_w(n) - y_g(n) = s_s(n) + (\mathbf{W}_o{}^{\Delta} \, \boldsymbol{n}(n))_1 - \, (\mathbf{G}_o{}^{\Delta} \, \boldsymbol{n}^{(i)}(n))_1 \tag{67}$$

From above equation, we see that the interference component is completely cancelled in the output $y_{GSC}(n)$.

6.3. The performance analysis

Since the QSWL GSC can totally remove the interference, its output signal-to-interference ratio (SIR) tends to infinite. Thus, we focus our attention on the output signal-to-noise ratio (*SNR*)

and array's gain. Let $\rho_n = \mathrm{E}\{|(\mathbf{W}_{\mathrm{o}}^{\Delta}\boldsymbol{n}(n))_1 - (\mathbf{G}_{\mathrm{o}}^{\Delta}\boldsymbol{n}^{(i)}(n))_1|^2\}$ is the power of output noise. From Eqs. (37) and (58), we have

$$(\mathbf{W}_{\mathrm{o}}^{\Delta}\boldsymbol{n}(n))_1 - (\mathbf{G}_{\mathrm{o}}^{\Delta}\boldsymbol{n}^{(i)}(n))_1 = (\mathbf{W}_1^H - \mathbf{G}_1{}^H)\boldsymbol{n}_1(n) + (\mathbf{W}_2^H + \mathbf{G}_2{}^H)\boldsymbol{n}_2(n) \tag{68}$$

Then, ρ_n can be written as

$$\rho_n = \sigma_n^2(\mathbf{W}_1^H - \mathbf{G}_1^H)(\mathbf{W}_1 - \mathbf{G}_1) + \sigma_n^2(\mathbf{W}_2^H + \mathbf{G}_2^H)(\mathbf{W}_2 + \mathbf{G}_2) \tag{69}$$

When the combined QPMC and MVDR are adopted in the second-stage beamformer, ρ_n can be written in the simple form (the proof is in Appendix D of Ref. [5])

$$\rho_n = \frac{\sigma_n^2}{\mu^2}(2M|P_s|^2\varepsilon^2 + |(P_i{}^{\Delta}P_s)_1|^2|\boldsymbol{q}_i^H\boldsymbol{q}_s|^2\lambda_q) \tag{70}$$

where $\lambda_q = \frac{\xi_i^{-2}|P_s|^2}{\kappa} - 2M|P_i|^2$, κ is given by Eq. (54). From Eq. (67), the expression of output SNR and array's gain A_q may be written as

$$SNR_{\mathrm{o}} = \xi_s\frac{(2M|P_s|^2\varepsilon - |(P_i{}^{\Delta}P_s)_1|^2|\boldsymbol{q}_i^H\boldsymbol{q}_s|^2)^2}{(2M|P_s|^2\varepsilon^2 + |(P_i{}^{\Delta}P_s)_1|^2|\boldsymbol{q}_i^H\boldsymbol{q}_s|^2\lambda_q)} \tag{71}$$

$$A_{\mathrm{q}} = \frac{(2M|P_s|^2\varepsilon - |(P_i{}^{\Delta}P_s)_1|^2|\boldsymbol{q}_i^H\boldsymbol{q}_s|^2)^2}{(2M|P_s|^2\varepsilon^2 + |(P_i{}^{\Delta}P_s)_1|^2|\boldsymbol{q}_i^H\boldsymbol{q}_s|^2\lambda_q)} \tag{72}$$

where ξ_s denotes the input signal-to-noise ratio (SNR) and ε is given by Eq. (43).

When the LCMV is adopted in the second-stage beamformer, ρ_n can be written in the simple form (the proof is in Appendix E of Ref. [5])

$$\rho_n = \frac{\sigma_n^2}{\mu^2}(2M|P_s|^2\varepsilon^2 + |(P_i{}^{\Delta}P_s)_1|^2|\boldsymbol{q}_i^H\boldsymbol{q}_s|^2\lambda_l) \tag{73}$$

where $\lambda_l = \frac{2M\xi_i^{-2}|P_s|^2}{\nu} - 2M|P_i|^2$, ν is given by Eq. (64). Then, the expression of output SNR and array's gain A_l may be written as

$$SNR_{\mathrm{o}} = \xi_s\frac{(2M|P_s|^2\varepsilon - |(P_i{}^{\Delta}P_s)_1|^2|\boldsymbol{q}_i^H\boldsymbol{q}_s|^2)^2}{(2M|P_s|^2\varepsilon^2 + |(P_i{}^{\Delta}P_s)_1|^2|\boldsymbol{q}_i^H\boldsymbol{q}_s|^2\lambda_l)} \tag{74}$$

$$A_l = \frac{(2M|P_s|^2\varepsilon - |(P_i{}^{\Delta}P_s)_1|^2|\boldsymbol{q}_i^H\boldsymbol{q}_s|^2)^2}{(2M|P_s|^2\varepsilon^2 + |(P_i{}^{\Delta}P_s)_1|^2|\boldsymbol{q}_i^H\boldsymbol{q}_s|^2\lambda_l)} \tag{75}$$

From Eqs. (71), (72), (74) and (75), we can see that the output SNR and array's gain depend on not only separation between the DOA's of the desired signal and interference (i.e., $|\boldsymbol{q}_i^H\boldsymbol{q}_s|$), but also difference between the polarizations of the desired signal and interference (i.e., $|(P_i^{\Delta}P_s)_1|$). The dependencies of them on $|\boldsymbol{q}_i^H\boldsymbol{q}_s|$ and $|(P_i{}^{\Delta}P_s)_1|$ are shown in following consequences:

1. When $|\boldsymbol{q}_i^H \boldsymbol{q}_s| = 0$, the separation between the DOAs of the desired signal and interference reaches to maximum. In this case, $A_{\mathrm{q}} = A_l = 2M|P_s|^2$. Further, $|\boldsymbol{q}_i^H \boldsymbol{q}_s|$ increases with a decrease of the DOA's separation. Thus, the array's gain A_{q} and A_l will reduce if $|P_s|^2$ is a constant. When $\boldsymbol{q}_i = \boldsymbol{q}_s$, $|\boldsymbol{q}_i^H \boldsymbol{q}_s| = 2M$. This implies that there is no separation between the DOAs of the desired signal and interference. In this case, the array's gain is given by

$$A_q = A_l = \frac{2M(|P_s|^2\varepsilon - 2M|(P_i{}^{\Delta}P_s)_1|^2)^2}{|P_s|^2\varepsilon^2 + 2M|(P_i{}^{\Delta}P_s)_1|^2\lambda} \tag{76}$$

where

$$\lambda = \frac{\xi_i^{-2}|P_s|^2}{2M(|P_s|^2|P_i|^2 - |(P_i{}^{\Delta}P_s)_1|^2)} - 2M|P_i|^2 \tag{77}$$

Further, $P_i = P_s$ if $\gamma_s = \gamma_i$ and $\eta_s = \eta_i$. Thus, the array's gain $A_q = A_l = 0$ due to $\lambda = \infty$. This implies that the QSWL GSC fails.

2. When $|(P_i{}^{\Delta}P_s)_1| = 0$, $A_q = A_l = 2M|P_s|^2$. In the cases that $\theta_s = \theta_i \neq 0$ and $\varphi_s = \varphi_i \neq 0$ (i.e., $\boldsymbol{q}_i = \boldsymbol{q}_s$), we have $|(P_i{}^{\Delta}P_s)_1| = (\sin^2\theta_s \cos^2\varphi_s + \sin^2\varphi_s)\cos(\gamma_i - \gamma_s)\cos(\eta_i - \eta_s)$. If $\gamma_i - \gamma_s = \pm\pi/2$ or $\eta_i - \eta_s = \pm\pi/2$, then $|(P_i{}^{\Delta}P_s)_1| = 0$. This implies that even though there is no separation between the DOAs of the desired signal and interference, the array's gain can also reach to $2M|P_s|^2$ by using the orthogonality between the polarizations of the desired signal and interference. Further, the array's gain decreases with an increase of $|(P_i{}^{\Delta}P_s)_1|$ if $|P_s|^2$ is a constant. When $P_i = P_s$, $|(P_i{}^{\Delta}P_s)_1| = |P_s|^2$. This implies that there is no difference between the polarizations of the desired signal and interference. But, the array's gain is not equal to zero if $\boldsymbol{q}_i \neq \boldsymbol{q}_s$.

In addition, the output *SNR* and array's gain depend also on the input *INR* ξ_i, the array's element number $2M$, the interference response's power $|P_i|^2$ and the desired signal response's power $|P_s|^2$.

7. Monte Carlo simulations

In this section, we investigate the performance of the proposed beamformers by two experiments. More results of simulations were shown in Refs. [2, 4, 5].

7.1. Experiment 1: the performance of QMVDR beamformer

In practice, if there is a misalignment between the desired signal's DOA and the look direction, the SINR of the complex MVDR beamformer degrades in the case of a scalar vector array [13]. In this experiment, we investigate the robustness of the beamformer against the DOA mismatch.

We consider each two-component vector-sensor has two orthogonal magnetic loop co-aligned along the x-axis, and assume that $M = 1$. The result is the average of the output SINR obtained by *1000* Monte Carlo runs. To compare the performance, the complex 'long vector' MVDR (CLVMVDR) [13], QMVDR and its INC beamformers are included in simulation results. For the CLVMVDR and QMVDR beamformers, the SINR is in general expressed in the form of logarithm. In order to be identical with the SINR of CLVMVDR and QMVDR beamformers, we define $SINR = 10\log\frac{\sigma_s^2}{\sigma_i^2+\sigma_n^2}$ in this experiment and assume that input $SINR = 0$ dB.

Figure 5 displays the output SINR as the function of the DOA error of the desired signal where the DOA error is between $-8°$ and $8°$. In the case of $\theta_s = 0°, \theta_i = 80°, \varphi_s = \varphi_i = 0°;$ $\gamma_s = \gamma_i = 60°, \eta_s = \eta_i = 30°,$ (i.e., the polarization of the desired signal and interference is identical, but the DOA is not identical), simulation results for two different sample sizes $N = 20$ and $N = 500$ are given in **Figure 5(a)** and **(b)**, respectively. From **Figure 5**, it is seen that the output *SINR* behaviour is different with different values of sample size N. In case of small N, as shown in **Figure 5(a)**, the INC and the QMVDR have a better robustness than the CLVMVDR. But the output *SINR* of the QMVDR and CLVMVDR is more than that of the INC. In case of large N, as shown in **Figure 5(b)**, the robustness against the DOA mismatch is almost identical for three beamformers. But the INC has the largest output *SINR* in three beamformers.

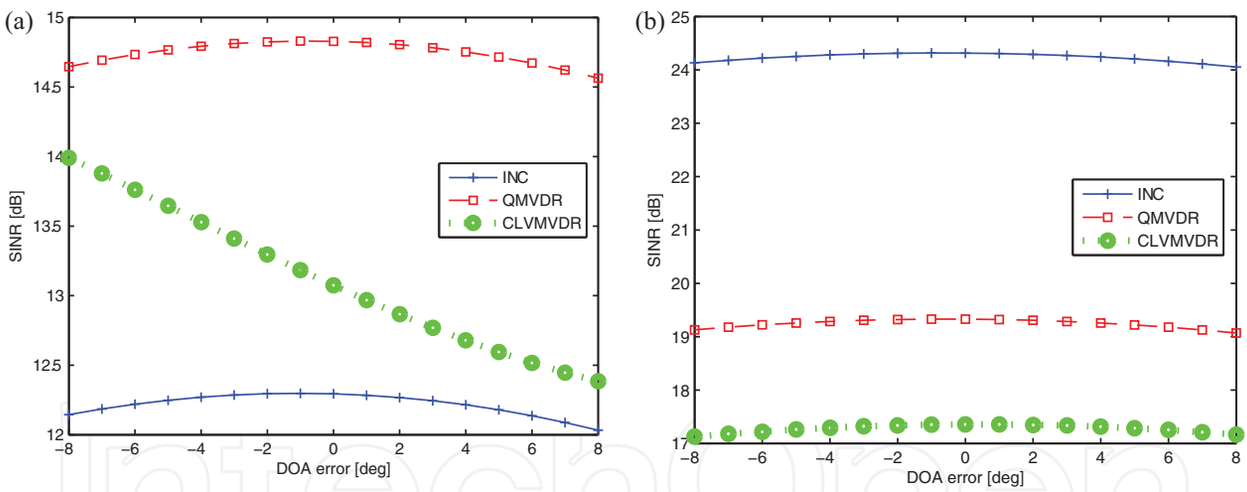

Figure 5. Output *SINR* against the DOA error.

7.2. Experiment 2: the performance of QSWL beamformer

In the second experiment, we illustrate the performance of the proposed QSWL GSC in the presence of a single interference. We assume $M = 6$, $\varphi_s = \varphi_i = 60°;$ $\gamma_s = \gamma_i = 30°, \eta_s = \eta_i = 30°,$ and that the covariance matrix $\mathbf{R}_x$, instead of $\mathbf{R}_{in}$, is available. **Figure 6** displays the power patterns for three values of $|\Delta\theta| :\ 60°,\ 20°$ and $10°$, where $\theta_s = |\Delta\theta|, \theta_i = 0°$. From **Figure 6**, it is seen that three beamformers steer almost a zero towards the interference's DOA (located at $0°$) in all cases. When $|\Delta\theta|$ decreases, the main-lobe of the QSWL GSC points almost to the source location, but the main-lobe of the complex 'long vector' LCMV (CLCMV) is away from

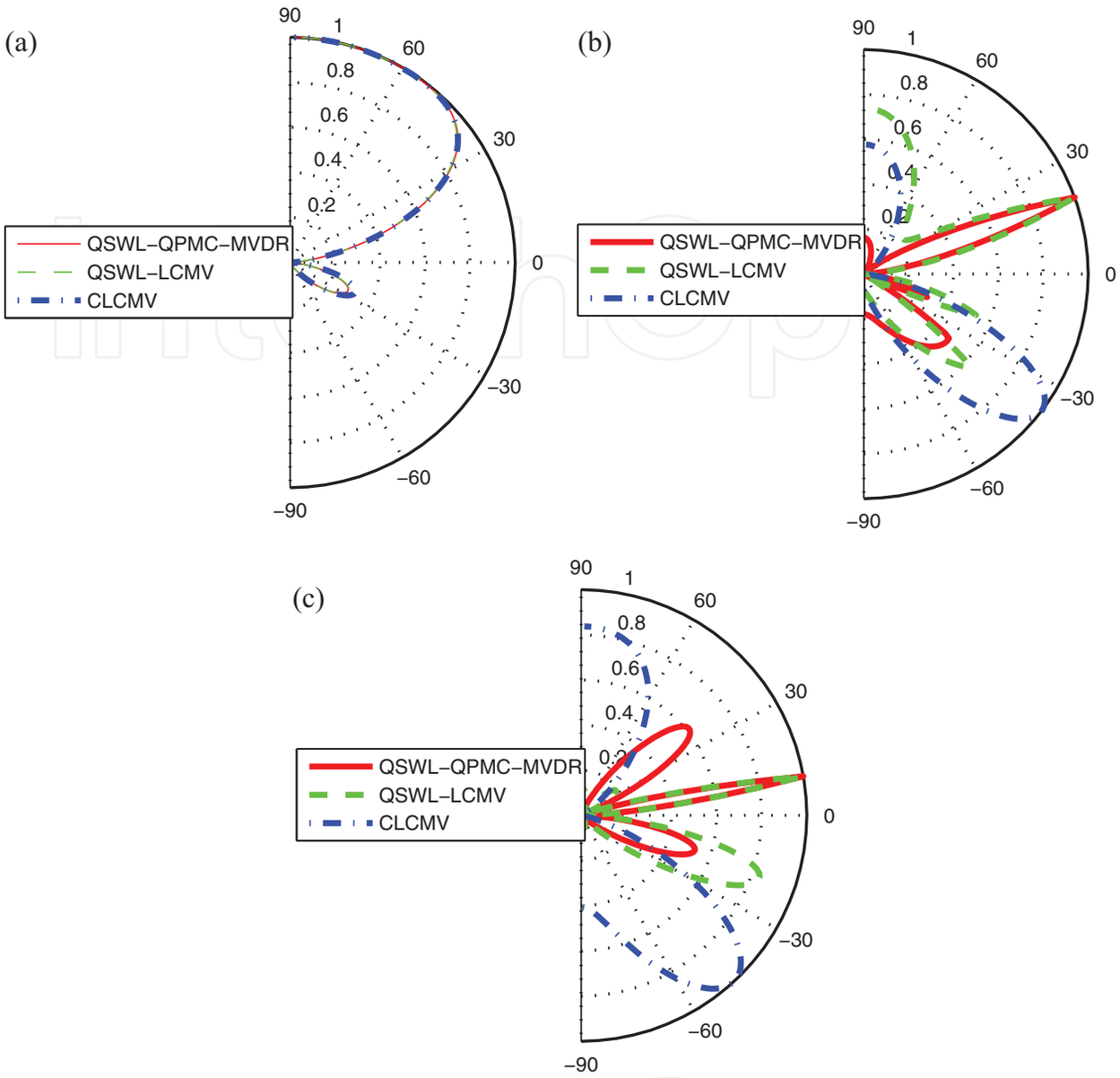

Figure 6. The power patterns at $\theta_s = |\Delta\theta|, \theta_i = 0^\circ$. (a) $|\Delta\theta| = 60^\circ$, (b) $|\Delta\theta| = 20^\circ$, (c) $|\Delta\theta| = 10^\circ$.

the source location. This implies that the QSWL GSC outperforms obviously CLCMV as the desired signal moves towards the interference. In addition, the side-lobes are amplified with a decrease of $|\Delta\theta|$. These side-lobes lead the beamformer to capture the white noise, which spans the whole space, so that the performance of beamformer degrades.

8. Conclusion

The problem of beamformer based on quaternion processes is considered in this chapter. The quaternion beamformers has more information than the complex 'long vector' beamformer.

The increase of information results in the improvement of the beamformer's performance. Analyses in theory and simulation results verify the advantages of quaternion beamformers.

Acknowledgements

This work was supported by the National Natural Science Foundation of China under Grants 61571462 and 60872088.

Author details

Jian-wu Tao[1,2] and Wen-xiu Chang[1,2]*

*Address all correspondence to: wenxiu_chang@gmail.com

1 Aviation University, Changchun, China

2 Jilin University, Changchun, China

References

[1] Tao, J.W., and Chang, W.X., "Quaternion MMSE Algorithm and Its Application In Beamforming", *Acta Aeronautica et Astronautica Sinica*, 2011, Vol. 32, no. 4, pp. 729–738.

[2] Tao, J.W., and Chang, W.X., "The MVDR Beamformer Based on Hypercomplex Processes", *Proc. 2012 IEEE International of Conference on Computer Science and Electronic Engineering*, Mar. 2012, pp. 273–277.

[3] Tao, J.W., and Chang W.X., "A Novel Combined Beamformer Based on Hypercomplex Processes", *IEEE Transactions on Aerospace and Electronic Systems*, 2013, Vol. 49, no. 2, pp. 1276–1288.

[4] Tao, J.W., "Performance Analysis for Interference and Noise Canceller based on Hypercomplex and Spatio-temporal-polarisation Processes", *IET Radar, Sonar and Navigation*, 2013, Vol. 7, no. 3, pp. 277–286.

[5] J.W. Tao, and W.X. Chang, "The Generalized Sidelobe Ganceller Based on Quaternion Widely Linear Processing", *The Scientific World Journal*, 2014, Vol. 2014, Article ID 942923, 12 pages.

[6] Mir, H.S., and Sahr, J.D., "Passive Direction Finding Using Airborne Vector Sensors in the Presence of Manifold Perturbations", *IEEE Transactions on Signal Processing*, 2007, Vol. 55, no. 1, pp. 156–164.

[7] Xiao, J.J., and Nehorai, A., "Optimal Polarized Beampattern Synthesis using a Vector Antenna Array", *IEEE Transactions on Signal Processing*, 2009, Vol. 57, no. 2, pp. 576–587.

[8] Nehorai A., Ho K.C., and Tan B.T.G., "Minimum-noise-variance Beamformer with an Electromagnetic Vector Sensor", *IEEE Transactions on Signal Processing*, 1999, Vol. 47, no. 3, pp. 601–618.

[9] Wong, K.T., "Blind Beamforming/Geolocation for Wideband-FFHs with Unknown Hop-Sequences", *IEEE Transactions on Aerospace and Electronic Systems*, 2001, Vol. 37, no. 1, pp. 65–76.

[10] Ward, J.P., *Quaternions and Cayley Numbers: Algebra and Applications*. Boston, MA: Kluwer, 1997.

[11] Mandic, D.P., Jahanchahi, C., and Took, C.C., "A Quaternion Gradient Operator and Its Applications," *IEEE Signal Processing letters*, 2011, Vol. 18, no. 1, pp. 47–50.

[12] Vía, J., Ramírez, D., and Santamaría, I., "Properness and Widely Linear Processing of Quaternion Random Vectors," *IEEE Transactions on Information Theory*, 2010, Vol. 56, no. 7, pp. 3502–351.

[13] Van Trees, H., *Optimum Array Processing (Detection Estimation, and Modulation Theory), Part IV*. New York: Wiley-Interscience, 2002.